

Hyperfine Structure of Hg^{193*} , Hg^{195} , and Hg^{195*} by Zeeman-Level Crossings*

WINTHROP W. SMITH†

*Department of Physics and Research Laboratory of Electronics, Massachusetts
Institute of Technology, Cambridge, Massachusetts*

(Received 6 April 1964; revised manuscript received 24 August 1964)

Hyperfine-structure measurements by optical detection of Zeeman-level crossings in the $6s6p\ ^3P_1$ state were made with natural-linewidth precision in three radioactive isotopes of mercury. The magnetic dipole (A) and electric quadrupole (B) interaction constants in Mc/sec implied by these measurements (without second-order hyperfine corrections, but including second-order Zeeman and cross-Zeeman hyperfine corrections) are:

| | |
|-------------------------------------|---|
| Hg^{195} (9.5-h half-life) | $A(^3P_1) = 15813.46 \pm 0.23$ |
| Hg^{195*} (isomer, 40 h) | $A(^3P_1) = -2368.04 \pm 0.08$ $B(^3P_1) = -782.45 \pm 0.86$ |
| Hg^{193*} (isomer, 11 h) | $A(^3P_1) = -2399.69 \pm 0.06$ $B(^3P_1) = -724.8 \pm 90.0$ |

The g_J factor for the 3P_1 state of Hg^{199} is obtained from a new level-crossing measurement. The value, including second-order Zeeman and Zeeman-hyperfine corrections, is $g_J = 1.486118 \pm 0.000016$; 37×10^{-6} of this is the total contribution from g_I and the second-order corrections. Our value is in substantial agreement with a recent measurement in the even Hg isotopes. The measured ratio of the A factors of Hg^{195} and Hg^{199} with all second-order corrections (resulting from interaction with neighboring fine-structure levels) included is combined with the value for the ratio of the magnetic moments in an external field obtained by Walter and Stavn to yield the Bohr-Weisskopf hfs anomaly between Hg^{195} and Hg^{199} , which is calculated to be $^{195}\Delta^{199}(^3P_1) = 0.1476(76)\%$. The contribution to the anomaly from the $s_{1/2}$ electron is extracted and used to estimate admixture coefficients in the single-particle model of the nucleus with configuration mixing. These turn out to be satisfactorily small for the configurations assumed.

INTRODUCTION

PRECISION measurements of the hyperfine-structure interaction constants in the $6\ ^3P_1$ state of three radioactive isotopes of mercury have been obtained by using optically detected Zeeman-level crossings. These measurements represent an increase in accuracy by a factor of approximately 100 over the previously available spectroscopic values for the magnetic-dipole interaction constants.^{1,2} This precision is sufficient to give information about the effects of the finite size of the distribution of magnetization in the nucleus.³ If the nuclear magnetic moments have not been measured directly, these measurements can serve as a guide for making precision measurements of the moments by optical pumping.^{4,5}

With the completion of the present work, double-resonance or level-crossing measurements of the hyperfine structure of mercury in the $6\ ^3P_1$ state are available

for the radioactive isotopes Hg^{193*} , Hg^{195} , Hg^{195*} , Hg^{197} , Hg^{197*} , and for the stable isotopes Hg^{199} and Hg^{201} .⁶ Since there are independent magnetic-moment data for Hg^{195} ,⁷ Hg^{197} ,⁸ Hg^{199} , and Hg^{201} ,⁸ one should be able to make a systematic comparison of the moments and hyperfine anomalies for these isotopes, using the shell model of the nucleus with configuration mixing.^{9,10}

The level-crossing technique was first used¹¹ to measure the fine structure of the $2\ ^3P$ state of helium. Essentially a rediscovery of the Hanle effect for large magnetic fields, this technique makes use of the change in the angular distribution of resonance fluorescence when two excited-state Zeeman sublevels become degenerate ("cross") in an applied magnetic field. The intensity resonances are quite sharp as a function of magnetic field, permitting calculation of the energy separations at zero field and hence the hyperfine structure, with a precision determined by the natural linewidth rather than by the Doppler width. The high precision obtainable with level crossings is also characteristic of the technique of optical double resonance,¹² although in this case it is necessary to produce population differences between magnetic sublevels in order

* This work, which is based on a Ph.D. thesis, Department of Physics, MIT, 1963, was supported in part by the U. S. Army, Navy, and Air Force under Contract DA-36-039-AMC-03200(E).

† Presently an NAS-NRC Postdoctoral Research Associate, National Bureau of Standards, assigned to the Joint Institute for Laboratory Astrophysics, Boulder, Colorado.

¹ W. J. Tomlinson III and H. H. Stroke, *J. Opt. Soc. Am.* **53**, 828 (1963); W. J. Tomlinson III, Ph.D. thesis, Department of Physics, M.I.T., 1963 (unpublished).

² H. Kleiman and S. P. Davis, *J. Opt. Soc. Am.* **53**, 822 (1963).

³ A. Bohr and V. F. Weisskopf, *Phys. Rev.* **77**, 94 (1950); F. Bitter, *ibid.* **76**, 150 (1949).

⁴ J. Brossel and A. Kastler, *Compt. Rend.* **229**, 1213 (1949).

⁵ W. T. Walter, *Bull. Am. Phys. Soc.* **7**, 295 (1962); W. T. Walter, Ph.D. thesis, Department of Physics, MIT, 1962 (unpublished).

⁶ F. Bitter, *Appl. Opt.* **1**, 1 (1962).

⁷ W. T. Walter and M. J. Stavn, *Bull. Am. Phys. Soc.* **9**, 10 (1964).

⁸ B. Cagnac, *Ann. Phys. (Paris)* **6**, 467 (1961).

⁹ H. H. Stroke, R. J. Blin-Stoyle, and V. Jaccarino, *Phys. Rev.* **123**, 1326 (1961).

¹⁰ A. Arima and H. Horie, *Progr. Theoret. Phys. (Kyoto)* **12**, 623 (1954).

¹¹ F. Colegrove, P. Franken, R. Lewis, and R. Sands, *Phys. Rev. Letters* **3**, 420 (1959).

¹² J. Brossel and F. Bitter, *Phys. Rev.* **86**, 308 (1952).

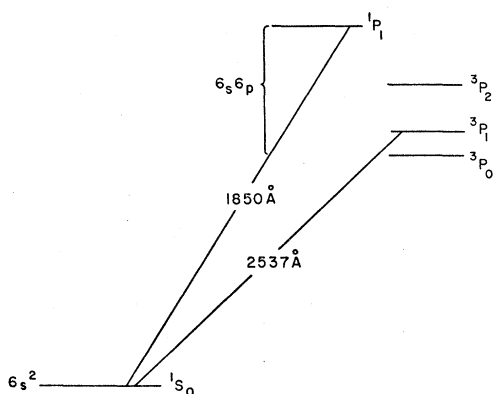


FIG. 1. Simplified mercury term diagram.

to observe the resonance. Level crossings in other isotopes of mercury have previously been observed by a number of workers,¹³⁻¹⁵ as well as crossings in zinc, cadmium, and lithium.¹⁶ The theory of level crossings has been worked out in detail by several workers.¹⁷

EXPERIMENT

Figure 1 shows the lowest lying energy levels in mercury. The 6^3P_1 state is excited by using the 2537-Å intercombination resonance line. The general features of a level-crossing experiment are illustrated in Fig. 2, which applies specifically to the 3P_1 state of an isotope with nuclear spin $I = \frac{1}{2}$ (for instance, Hg¹⁹⁹ or Hg¹⁹⁵). Each of the hyperfine levels is split by the applied magnetic field. Two of the Zeeman sublevels ($F = \frac{3}{2}$, $m_F = -\frac{3}{2}$ and $F = \frac{1}{2}$, $m_F = +\frac{1}{2}$) become degenerate at a value of the applied field given approximately by

$$g_J \mu_0 H_+ / A \approx 1, \quad (1)$$

where g_J is the gyromagnetic ratio for the 3P_1 state, μ_0 the Bohr magneton, H_+ the magnetic field at the crossing, and A the magnetic dipole interaction constant. Equation (1) can be obtained by solving the secular equation for each of the two magnetic substates that cross, by using the perturbation Hamiltonian¹⁸

$$\mathcal{H} = A \mathbf{I} \cdot \mathbf{J} + B Q_{op} + \mu_0 (g_J \mathbf{J} - g_I \mathbf{I}) \cdot \mathbf{H}. \quad (2)$$

[Here g_J and g_I are each expressed in terms of the Bohr magneton; $\langle Q_{op} \rangle = 0$ when $I \leq \frac{1}{2}$; therefore, B does not enter into (1).] It is clear from (1) that a measurement

¹³ H. R. Hirsch and C. V. Stager, *J. Opt. Soc. Am.* **50**, 1052 (1960); H. R. Hirsch, *ibid.* **51**, 1192 (1961).

¹⁴ J. N. Dodd, *Proc. Phys. Soc. (London)* **77**, 669 (1961).

¹⁵ R. D. Kaul, Ph.D. thesis, Department of Physics, Case Institute of Technology, 1963 (unpublished).

¹⁶ A. Landman, P. Thaddeus, and R. Novick, *Bull. Am. Phys. Soc.* **7**, 26 (1962); P. Thaddeus and R. Novick, *Phys. Rev.* **126**, 1774 (1962); K. Brog, Ph.D. thesis, Department of Physics, Case Institute of Technology, 1963 (unpublished).

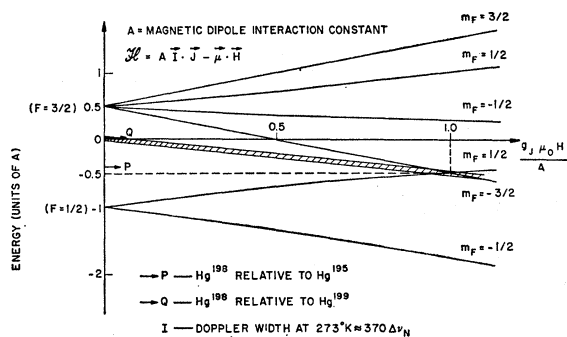
¹⁷ P. Franken, *Phys. Rev.* **121**, 508 (1961); M. E. Rose and R. L. Carovillano, *ibid.* **122**, 1185 (1961); G. Breit, *Rev. Mod. Phys.* **5**, 91 (1933); see especially pp. 117-125.

¹⁸ H. Kopfermann, *Nuclear Moments* (Academic Press Inc., New York, 1958).

of the field H_+ is tantamount to measuring the ratio g_J/A , so that if g_J is already known (from a measurement on another isotope), we can obtain A .

Observation of the crossing field is made possible by illuminating the sample (in vapor form) with 2537-Å resonance radiation whose frequency has been Zeeman shifted slightly¹⁹ to be in optical resonance with the levels at the crossing point. The Doppler width of the lamp is represented in Fig. 2 by the cross-hatched band, and the necessary isotope shift for illuminating the crossings in Hg¹⁹⁹ and Hg¹⁹⁵ by the positions of arrows P and Q . The isotope shift relative to Hg¹⁹⁸, as well as approximate A values for each isotope, were available from previous spectroscopic work¹; this greatly facilitated proper Zeeman shifting of the lamp and location of the level-crossing point.

The apparatus, which is patterned after that used by Hirsch,¹³ is shown schematically in Fig. 3. Quartz lenses and cells are used throughout to transmit the 2537-Å line. Light from an electrodeless Hg¹⁹⁸ lamp, located inside the Zeeman-scanning magnet, passes through a collimating lens and a quarter-wave plate-polarizer combination (which passes only one component of the Zeeman triplet from the lamp when the light emerges parallel to the scanning field) into the cell containing the radioactive mercury vapor. The cell (a 1-cm cube) is placed in the gap of a Harvey-Wells 12-in. magnet. Light scattered (at 90°) from the radioactive vapor (density $\sim 10^{18}$ atoms/cc) is monitored by a 1P28 photomultiplier and its intensity recorded as the magnetic field ("splitting field") is slowly swept through the value H_+ . The curve of intensity versus field has roughly Lorentzian shape.¹⁷ Small-amplitude field modulation and phase-sensitive detection are used to increase sensitivity, thereby giving a recorder tracing that looks like the derivative of a Lorentzian curve. No filters for the 2537-Å line are needed, since the mercury vapor cell acts as its own filter. The solid angle for the light scattered by the cell into the photomultiplier was limited to approximately 0.01 sr.


 FIG. 2. Hyperfine levels in a magnetic field for $J = 1$, $I = \frac{1}{2}$.

¹⁹ F. Bitter, H. Plotkin, B. Richter, A. Teviotdale, and J. E. R. Young, *Phys. Rev.* **91**, 421 (1953).

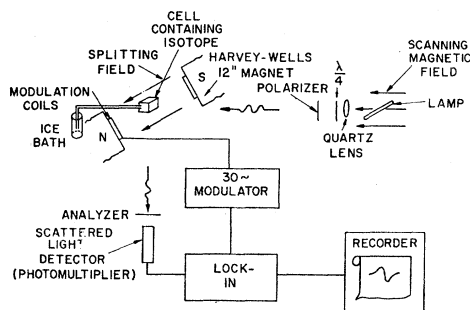


FIG. 3. Experimental arrangement for level-crossing work.

The scanning magnet for the lamp (see Fig. 3) is a commercial unit built to our specifications,²⁰ and has a maximum field of ~ 11 kG.

All of the isotopes were produced by the reaction $\text{Au}^{197}(p, xn)\text{Hg}^{198-x}$; internal bombardments with protons in the energy range 30–50 MeV were carried out at the Harvard University cyclotron. Beam current was $\lesssim 1 \mu\text{A}$, requiring bombardment times of 6–8 h on a $1 \text{ cm} \times 5 \text{ cm} \times 0.006 \text{ in.}$ gold-foil target. Target probe positions were determined in order to optimize the production of the desired isotopes for each run at the expense of the others. The isotopic composition of each sample was verified for each cyclotron energy by high-resolution optical spectroscopy and gamma-ray spectroscopy.¹ The procedure for transferring the radioactive mercury from the target foil was essentially the same as that used by Melissinos.²¹

The magnetic field was measured in the vicinity of the crossing by using a proton-resonance probe.²² Since the cell and resonance probe were not at the same point in the field, it was necessary to reduce the difference in field between them to zero or to obtain an estimate of this small field difference. The most satisfactory arrangement of cell and probe was to place them in symmetrical positions about the center of the magnet gap. The residual correction, estimated to be approximately 1:60 000 or less, was difficult to measure accurately because of fluctuations in the magnet current of the same order of magnitude. A method is suggested in Appendix C for measuring small field differences in the presence of fluctuating magnetic fields by using two magnetic resonance probes connected in parallel.

²⁰ The magnet (Model UFS-1) was built by Magnion, Inc., Cambridge, Massachusetts. It is roughly a cube, 8 in. on a side, and weighs approximately 100 lb.

²¹ A. C. Melissinos, *Phys. Rev.* **115**, 126 (1959).

²² Probe was similar to the Harvey-Wells Type-124 magnetic-resonance probe. Proton resonance frequencies in Mc/sec were converted to units of $\mu_0 H$ in Mc/sec using the conversion factor 328.7319 ± 0.0006 derived in Appendix A of Kaul's thesis (Ref. 15). This takes into account an approximate diamagnetic correction due to probe composition and cylindrical shape. This conversion factor is consistent with the value of the Bohr magneton-proton magnetic moment ratio obtained by Hardy and Purcell [see J. H. Sanders, *The Fundamental Atomic Constants* (Oxford University Press, London, 1961), p. 52, referring to W. A. Hardy, *Bull. Am. Phys. Soc.* **4**, 37 (1959)].

TABLE I. Measured proton resonance frequencies for level crossings.^a (Mean values normalized as indicated in Appendix B; except for Hg^{199} , errors are three times the standard deviation of the mean.)

| Isotope | Crossing | Frequency ^b (kc/sec) |
|---|--|------------------------------------|
| Hg^{196} ($I = \frac{1}{2}$) | $F = \frac{3}{2}, m_F = -\frac{3}{2}$ $F = \frac{1}{2}, m_F = \frac{1}{2}$ | 32370.06 ± 0.45 |
| Hg^{195*} ($I = \frac{13}{2}$) | $F = \frac{15}{2}, m_F = \frac{15}{2}$ $F = \frac{13}{2}, m_F = \frac{11}{2}$ | 33926.4 ± 1.1 |
| | $F = \frac{13}{2}, m_F = \frac{11}{2}$ $F = \frac{13}{2}, m_F = \frac{7}{2}$ | 32682.6 ± 0.8 |
| | $F = \frac{13}{2}, m_F = \frac{9}{2}$ $F = \frac{13}{2}, m_F = \frac{5}{2}$ | 31580.7 ± 8.7 |
| Hg^{195*} ($I = \frac{13}{2}$) | $F = \frac{15}{2}, m_F = \frac{15}{2}$ $F = \frac{13}{2}, m_F = \frac{11}{2}$ | 34380.51 ± 0.42 |
| Hg^{199} ($I = \frac{1}{2}$) (Calibration.) | $F = \frac{3}{2}, m_F = -\frac{3}{2}$ $F = \frac{1}{2}, m_F = \frac{1}{2}$ | 30197.95 ± 0.23 |

^a Preliminary results for Hg^{196} and Hg^{195*} have appeared previously: W. W. Smith, *Bull. Am. Phys. Soc.* **8**, 9 (1963).

^b See Ref. 22.

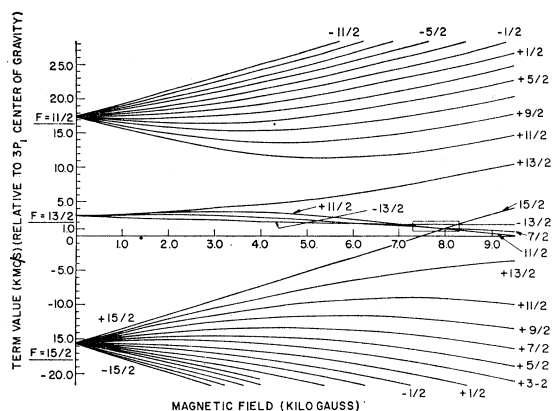
RESULTS

Proton-Resonance Frequencies for Level Crossings

A summary of the observed level-crossing data is given in Table I. The crossings observed in Hg^{195*} ($I = 13/2$) may be identified from the Zeeman diagrams (Figs. 4 and 5). The Zeeman diagram for Hg^{195*} (also $I = 13/2$) is similar to that for Hg^{196*} , although the detailed positions of the crossings in this isotope are uncertain because only one crossing was observed. Figure 6 shows some sample recorder tracings obtained by field modulation. In searching for a crossing, the modulation amplitude was adjusted to produce maximum signal²³ and then reduced to narrow the linewidth when making measurements.

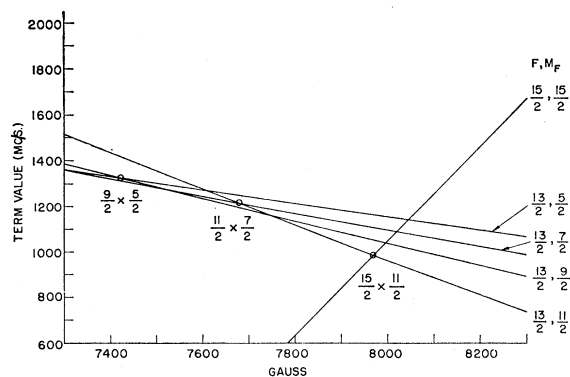
The search for each crossing and identification of the associated Zeeman levels was facilitated by the availability of spectroscopic data on the hyperfine structure

²³ H. Wahlquist, *J. Chem. Phys.* **35**, 1708 (1961).

FIG. 4. Zeeman pattern of Hg^{195*} (40 h).

for each isotope,¹ which permitted a prediction of the approximate positions of the crossings. In the case of Hg^{195*} in which three crossings were observed, the main (narrow) crossing ($F=15/2$, $m_F=15/2 \times F=13/2$, $m_F=11/2$) was identified by its width and by the fact that its implied A value agreed with the spectroscopic value for A . The two broader crossings can be identified partly by width and intensity, but most convincingly by the fact that their approximate positions can be calculated from the A value obtained from the first crossing (which is relatively insensitive to B) and the spectroscopic B value. The assignments of levels for these crossings are the only ones that correspond to $|\Delta m_F|=2$ and are consistent with the spectroscopic data. Furthermore, the position of the third crossing for Hg^{195*} listed in Table I, predicted by using the known value of g_J for the 3P_1 state and the A and B values obtained from the first two crossings alone, agrees with observation. One may also consider the consistency of the three crossings as a confirmation of the measurement of the nuclear spin as $13/2$.¹

The values given in Table I were obtained by using the ratio of the measured frequency for any given crossing to the proton-resonance frequency for the single crossing in Hg¹⁹⁹. The frequency ratios were

FIG. 5. Detail of level crossings in Hg^{195*} between 7300 and 8300 G.

found to be more consistent from run to run than the absolute frequencies, probably because small cell-to-probe corrections cancel out of the frequency ratios. These ratios were obtained separately for each run and then averaged. The “normalized means” (the mean-frequency ratio multiplied by the mean proton-resonance frequency for the Hg¹⁹⁹ crossing) of all runs fall within the error limits given, which in general are three times the standard deviation of the mean. The data are presented in detail in Appendix B.

An attempt was made to seek out sources of systematic error. The shifts in the position of the center of a level crossing resulting from the finite lock-in time constant and sweep time have been discussed by Novick.²⁴ For a small ratio of lock-in time constant to sweep time, the shift is linear and should cancel out of the mean if an equal number of up-field and down-field sweeps are included. For the sinusoidal field modulation used here, there is no shift of the center of the line but merely a broadening that is due to the finite modulation amplitude.²⁵ No significant shifts were observed when the lamp power was changed slightly, or when the lamp frequency was detuned from optical resonance.

Hyperfine-Interaction Constants

Values of the magnetic dipole and electric quadrupole interaction constants, calculated from the values in Table I, are given in Table II. The A value for Hg¹⁹⁵ is obtained from the Hg¹⁹⁵-Hg¹⁹⁹ proton-resonance frequency ratio and the accurately known A value for Hg¹⁹⁹.²⁵ Second-order Zeeman and cross Zeeman-hyperfine corrections have been applied to get the “low-field” values of A_{195}/A_{199} and the “low field” A

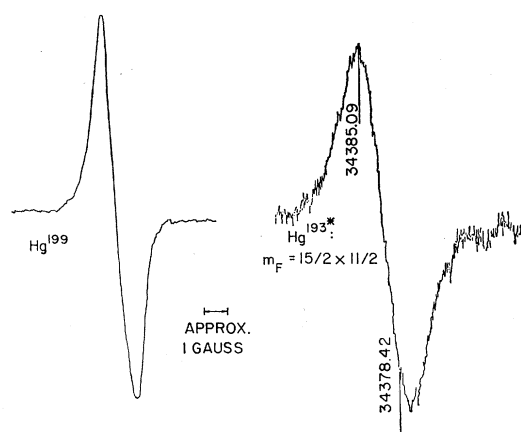


FIG. 6. Typical recorder tracings for level crossings observed by using field modulation. Integrating time: 1–3 sec. Lines are broadened by a factor ~ 3 by finite field modulation amplitude; modulation was set to maximize the signal.

²⁴ R. Novick, Quarterly Progress Report, Columbia University Radiation Laboratory, 1961 (unpublished).

²⁵ C. V. Stager, Phys. Rev. **132**, 275 (1963).

TABLE II. Values of the hyperfine interaction constants.

| Quantity | Spectroscopic results ^a | Present work "Low-field" constants. Second-order Zeeman and cross Zeeman-hyperfine corrections included | Present work "Isolated" constants. All second-order corrections included |
|--------------------|------------------------------------|---|---|
| $A_{195}(^3P_1)$ | 15838±130 Mc/sec | 15813.46±0.23 Mc/sec | 15815.56±0.24 Mc/sec |
| $A_{196}(^3P_1)$ | ... | 1.071927±0.000015 | 1.071936±0.000018 |
| $A_{199}(^3P_1)$ | ... | ... | ... |
| $A_{195}^*(^3P_1)$ | -2367±7 | -2368.04±0.08 Mc/sec | -2367.98±0.08 Mc/sec |
| $B_{195}^*(^3P_1)$ | -794±90 | -782.45±0.86 | -777.97±0.86 |
| $A_{198}^*(^3P_1)$ | -2394±11 | -2399.69±0.07 ^b | -2399.63±0.07 ^b |
| $B_{198}^*(^3P_1)$ | -749±150 | -724.8 ±90.0 ^c | -720.2 ±90.0 ^c |

^a W. J. Tomlinson, III and H. H. Stroke, see Quarterly Progress Report No. 66, Research Laboratory of Electronics, MIT, 1962, p. 18 (unpublished); and W. J. Tomlinson, III, Ph.D. thesis, Department of Physics, M.I.T., 1963 (unpublished).

^b Preliminary value: it is assumed that $B = -749 \pm 150$ Mc/sec.

^c Least-squares fit to all available spectroscopic and level-crossing data. Only one level-crossing measurement for this isotope was available, hence the large uncertainty in B . The crossing observed is much more sensitive to A than to B .

and B values listed in Table II. These represent the experimental values for these quantities which could be measured by direct hyperfine transitions in small fields. Second-order hyperfine corrections, independent of magnetic field, are included in the "isolated" A and B values of Table II; these should be used in hfs anomaly calculations. The A and B constants were determined by a least-squares fit to the data, through use of the program HYPERFINE-4, modified to permit calculation of the second-order corrections.²⁶

Second-Order Corrections and g_J

The magnetic field for a level crossing between sub-levels of a state with $J=1$ is given approximately by $A = g_J \mu_0 H_+$ when $I = \frac{1}{2}$. Thus the ratio of the A factors is very nearly the ratio of the proton-resonance frequencies for the crossings in the two isotopes. This statement is exact if g_I/g_J is vanishingly small and if there are no other fine-structure states nearby with the same (m_F) values as the crossing levels to perturb the energies.

To retain the full precision of the data, one must apply second-order Zeeman and Zeeman-hyperfine corrections in intermediate coupling^{27,28} when calculating an expression for the level-crossing field in terms of A . The first-order energies of an isolated hyperfine multiplet in a magnetic field are calculated by diagonalization of the matrix of the hyperfine Hamiltonian (2). Here we consider only states belonging to a single fine-structure level. When the perturbations from

neighboring fine-structure levels are included, it turns out that there are off-diagonal matrix elements of the Zeeman and hyperfine interactions between different fine-structure states. The final values of the term energies with second-order corrections are obtained by diagonalizing the submatrix for the fine-structure state of interest, after making a Van Vleck transformation on the complete matrix for the $6s6p$ configuration which eliminates the off-diagonal elements between different fine-structure states to second order.^{15,29}

The procedure just described, when applied to the level crossing in the 3P_1 state of an isotope with $I = \frac{1}{2}$, yields³⁰

$$\begin{aligned}
 A = g_J' \mu_0 H_+ & \left(1 - \frac{g_I}{2g_J} \right) + \frac{\alpha^2 \mu_0^2 H_+^2}{24} \left(\frac{8}{\delta_0} + \frac{3\beta^2}{\delta_1} - \frac{1}{\delta_2} \right) \\
 & + \frac{39}{288} \frac{\alpha \beta \mu_0 H_+}{\delta_1} \left\{ -3c_1 c_2 a_3 + 5 \left(c_1 c_2 + \frac{c_1^2 - c_2^2}{4\sqrt{2}} \xi \right) a_{3/2} \right. \\
 & \left. - 2c_1 c_2 a_{1/2} \right\} + \frac{\alpha \mu_0 H_+}{6^{1/2} \delta_0} \left\{ c_2 (a_s - a_{1/2}) - c_1 \frac{5\sqrt{2}}{8} \xi a_{3/2} \right\} \\
 & - \frac{\sqrt{3}}{6} \frac{\alpha \mu_0 H_+}{\delta_2} \left\{ c_1 a_s - \left(c_1 + c_2 \frac{5\sqrt{2}}{8} \xi \right) a_{3/2} \right\}. \quad (3a)
 \end{aligned}$$

A in this expression is what would be measured by double resonance in low external field. The constant g_J' is the gyromagnetic ratio for the 3P_1 state which would be measured in an even Hg isotope at low field.

²⁶ We are grateful to Professor H. Shugart, Lawrence Radiation Laboratory, University of California, Berkeley, for the original version of this program. The modifications to include the second-order corrections were made by Dr. P. Thaddeus; the first use of this program is reported in P. Thaddeus and M. N. McDermott, Phys. Rev. **132**, 1186 (1963).

²⁷ M. N. McDermott and W. L. Lichten, Phys. Rev. **119**, 134 (1960).

²⁸ A. Lurio, M. Mandel, and R. Novick, Phys. Rev. **126**, 1758 (1962).

²⁹ E. C. Kemble, *The Fundamental Principles of Quantum Mechanics with Elementary Applications* (Dover Publications, Inc., New York, 1937), p. 394 ff.

³⁰ This expression applies to a positive magnetic moment ($A > 0$) so that the levels that cross are $(\frac{3}{2}, m_F) = (\frac{3}{2}, -\frac{3}{2})$ and $(\frac{1}{2}, \frac{1}{2})$. If the moment is negative, then the crossing levels are $(\frac{3}{2}, \frac{3}{2})$ and $(\frac{1}{2}, -\frac{1}{2})$ and (3) is transformed into the appropriate expression by changing the sign of H_+ , in agreement with Thaddeus and Novick [Phys. Rev. **126**, 1774 (1962)].

The expansion coefficients α , β , and c_1 , c_2 express the "³P₁" state wave function in terms of pure *LS* and *jj* wave functions, respectively. a_s , $a_{1/2}$, $a_{3/2}$ are the single-electron hyperfine interaction constants.¹⁸ ξ has been defined by Schwartz.³¹ The fine-structure energy denominators are:

$$\begin{aligned}\delta_0 &= E(^3P_1) - E(^3P_0), \\ \delta_1 &= E(^1P_1) - E(^3P_1), \\ \delta_2 &= E(^3P_2) - E(^3P_1).\end{aligned}$$

The numerical values used in evaluating (3a) and in the computer calculation of second order corrections for the other isotopes are given in Table III.

Making the substitution,

$$y \equiv A/\mu_0 H_+ - g_J' [1 - (g_I/2g_J')],$$

(3a) can be written:

$$A = g_J' \mu_0 H_+ [1 - (g_I/2g_J')] + \mu_0 H_+ y. \quad (3b)$$

From this we obtain the ratio of the *A* factors for Hg¹⁹⁵ and Hg¹⁹⁹ in terms of the ratio of the level-crossing fields:

$$\begin{aligned}\frac{A(195)}{A(199)} &= \frac{H_+(195)(g_J - \frac{1}{2}g_I + y)_{195}}{H_+(199)(g_J - \frac{1}{2}g_I + y)_{199}} \\ &\approx \frac{H_+(195)}{H_+(199)} \left(1 - \frac{\Delta g_I}{2g_J} + \frac{\Delta y}{g_J} \right) \\ &= \frac{\nu_{\text{proton}}(195)}{\nu_{\text{proton}}(199)} (1 - 13.1 \times 10^{-6} + 11.3 \times 10^{-6}) \\ &= \frac{\nu_{\text{proton}}(195)}{\nu_{\text{proton}}(199)} (1 - 1.8 \times 10^{-6}).\end{aligned} \quad (4)$$

In this case, fortuitously, the g_I and second-order corrections nearly cancel out of the ratio.

The experimental value³² for the proton-resonance frequency ratio for the crossings in Hg¹⁹⁵ and Hg¹⁹⁹ is $\nu_p(195)/\nu_p(199) = 1.071929(15)$ (see Appendix B) which leads to

$$\begin{aligned}A(195)/A(199) &= 1.071929(15) \times (1 - 1.8 \times 10^{-6}) \\ &= 1.071927(15).\end{aligned} \quad (5)$$

Since the *A* factor for Hg¹⁹⁹ is known,²⁵ Eq. (3a) can be used, together with the H_+ for Hg¹⁹⁹, to calculate g_J' for the ³P₁ state. Although a preliminary g_J value has been given previously for Hg¹⁹⁹ with high precision,¹⁵ it is of some interest to report the value obtained here in view of a small disagreement with this earlier value, for which no explanation has yet been found. Using

³¹ C. Schwartz, Phys. Rev. **97**, 380 (1955).

³² The notation 1.071929(15) means 1.071929 ± 0.000015; that is, the number in parentheses represents the uncertainty in the last place.

TABLE III. Constants used in second-order corrections. Symbols are defined in the text, or in Ref. 28. The symbols α , β [$= -(1-\alpha^2)^{1/2}$], c_1 , and $c_2 = (1-c_1^2)^{1/2}$ were calculated to be consistent with the measured value of g_J' , using formulas given in Table IV of Ref. 28. The single electron dipole interaction constants for Hg¹⁹⁹ were calculated in the manner of Ref. 27 from $A(^3P_1)_{199}$, $A(^3P_2)_{199}$ and the theoretical value for $a_{1/2}/a_{3/2}$. The single-electron constants for the radioactive isotopes were then derived from the Hg¹⁹⁹ constants by the method outlined in Ref. 25. The quantity $b_{3/2}$ was calculated from $B(^3P_1)$ for the same isotope according to Eq. (13) of Ref. 28. The uncertainties in $a_{1/2}/a_{3/2}$ and the neglect of hfs anomalies (typically ~0.1% in Hg) suggest that the single-electron interaction constants should be reliable to ~1%,^a sufficient accuracy to obtain the corrected *A*'s and *B*'s to within the experimental uncertainties.

| | | | | |
|-------------------------|--------------------------|--------------------------|---------------------------|---------------------------|
| g_J' | 1.486118 | $A(^3P_1)_{199}^c$ | 14 752.37 Mc/sec | |
| α | 0.98488 | $A(^3P_2)_{199}^c$ | 9066.62 Mc/sec | |
| c_1 | 0.42717 | δ_0^d (Mc/sec) | 0.5298 × 10 ⁸ | |
| ξ^a | 1.094 | δ_1^d (Mc/sec) | 4.3939 × 10 ⁸ | |
| η^a | 1.354 | δ_2^d (Mc/sec) | 1.3882 × 10 ⁸ | |
| $a_{1/2}/a_{3/2}^{a,b}$ | 11.52 | | | |
| Isotope: | 199 | 195 | 195* | 193* |
| a_s (Mc/sec) | 34969 | 37484 | -5614 | -5689 |
| $a_{3/2}$ (Mc/sec) | 432.6 | 463.7 | -69.45 | -70.38 |
| $b_{3/2}$ (Mc/sec) | ... | ... | +1216 | +1186 |
| g_I | 0.542 × 10 ⁻³ | 0.581 × 10 ⁻³ | -0.870 × 10 ⁻⁴ | -0.882 × 10 ⁻⁴ |

^a M. N. McDermott and W. L. Lichten, Phys. Rev. **119**, 134 (1960).

^b R. D. Kaul, Ph.D. thesis, Case Institute of Technology, 1963 (unpublished).

^c Reference 25.

^d Charlotte E. Moore, *Atomic Energy Levels* (U. S. Government Printing Office, Washington, D. C., 1958), Vol. III, p. 192.

the mean value of the proton-resonance frequency for the Hg¹⁹⁹ crossing given in Table I, we find from (3a) that $g_J' = 1.486118(16)$, of which $+3.7 \times 10^{-5}$ is the contribution from g_I and the second-order corrections. A comparison among some values for g_J' recently obtained is given in Table IV. The values for g_J' in Hg¹⁹⁹ were all calculated by using Stager's precision measurement of $A(^3P_1)$ in this isotope.²⁵ Similarly, the values for g_J' in Hg²⁰¹ are based on Kohler's precision measurement of $A(^3P_1)$ in Hg²⁰¹.⁶ (The self-consistency of Kaul's results¹⁵ for g_J' in Hg¹⁹⁹ and Hg²⁰¹ indicates that the *A* values for Hg¹⁹⁹ and Hg²⁰¹ are probably consistent within Kaul's stated error.) There is a discrepancy of a few parts per million between Kaul's value for g_J' and the value obtained here.³³ While the even-isotope value of Kohler and Thaddeus³⁴ is just consistent with our value, there appears to be a definite discrepancy of approximately 2:10⁵ between Kaul's value and that of Kohler and Thaddeus.

As far as our measurement is concerned, it is possible that some small systematic errors of a few parts per million are present because of the difficulty in measuring the cell-to-probe field difference (see Appendix C and Ref. 34). Nonetheless, as indicated in Appendix B, the error limits for $H_+(199)$ were chosen to encompass the

³³ A new preliminary measurement of H_+ for Hg¹⁹⁹ by O. Redi, National Magnet Laboratory, M.I.T., gives a proton-resonance frequency (for 0.01M FeCl₃ solution) of 30198.14 ± 0.15 kc/sec, in agreement with our value. This leads to a corrected $g_J' = 1.486107(12)$. The magnet that was used had a current stability of 1:10⁶. O. Redi (private communication).

³⁴ R. Kohler and P. Thaddeus, Phys. Rev. **134**, A1204 (1964).

TABLE IV. Some recent measurements of $g_J(^3P_1)$ in mercury.^a

| Isotope | Method of measurement | g_J | Reference |
|---------|-----------------------------|---------------|-------------------------------|
| Even | High-field double resonance | 1.486094(8) | Kohler and Thaddeus (Ref. 34) |
| | | 1.486118(16) | Smith (this paper) |
| 199 | Level crossing | 1.486147(10) | Kaul (Ref. 15) |
| | Level crossing | 1.486165(50) | Dodd (Ref. 14) ^b |
| | Level crossing | 1.486156(18) | Kaul (Ref. 15) |
| | Level crossing | 1.486030(130) | Dodd (Ref. 14) ^b |
| 201 | | | |

^a Values are corrected in the same way for g_I and second-order Zeeman and fine-structure effects.

^b Recalculated from the data using Kaul's second-order corrections.

means of several runs taken under a variety of conditions which would be expected to affect the cell-to-probe correction in a more or less random fashion. A brass light pipe in the apparatus, suspected because of possible magnetic impurities, was found to produce no shift of the field in the magnet to within $1:10^5$ or less.

Hyperfine Anomaly for Hg¹⁹⁵ and Hg¹⁹⁹

Although the magnetic dipole interaction constant A is approximately proportional to the nuclear g factor (g_I), the ratio of the A factors for two isotopes, in general, deviates slightly from the ratio of the g_I 's.³ The quantity

$${}^1\Delta^2 \equiv A_{1g_2}/A_{2g_1} - 1, \quad (6)$$

frequently referred to as the hyperfine-structure anomaly, can be calculated when the ratios of the A factors and the g factors are measured independently.

For comparison of the anomaly with theory, it is desirable not to use the experimental A factors in (6), since the A factor for the "³ P_1 " state includes contributions from the ³ P_2 , ³ P_0 and ¹ P_1 fine-structure levels. To get the anomaly for the isolated ³ P_1 state (which will be used to calculate the anomaly for a single electron), we calculate the second-order hyperfine corrections²⁸ and subtract them from the "low-field" A factors before using (6). The corrections to be subtracted are

$$\delta A_{195} = -2.10 \text{ Mc/sec},$$

$$\delta A_{199} = -1.83 \text{ Mc/sec},$$

so the corrected (or "isolated") A factors become

$$\begin{aligned} A_{195}'(^3P_1) &= 15\,815.56(24) \text{ Mc/sec}, \\ A_{199}'(^3P_1) &= 14\,754.20(2) \text{ Mc/sec}. \end{aligned} \quad (7)$$

Using these values in (6), together with the ratio of the nuclear g factors $g_{195}/g_{199} = 1.070356(66)$ reported by Walter and Stavn,⁷ we obtain

$${}^{195}\Delta^{199}(^3P_1) = 0.1476(76)\%. \quad (8)$$

The theory of hyperfine-structure anomalies as worked out by Bohr and Weisskopf⁸ is in terms of the anomaly for the individual $s_{1/2}$ and $p_{1/2}$ electrons. The anomaly for the $s_{1/2}$ electron [$\Delta(s_{1/2})$] can be expressed in terms of $\Delta(^3P_1)$ if we break up the A factors into individual

electron contributions.^{25,27} Using the single-electron A factors and intermediate coupling coefficients from Table III and assumptions similar to those of Stager,²⁵ we estimate that

$${}^{195}\Delta^{199}(s_{1/2}) = 1.141(20){}^{195}\Delta^{199}(^3P_1). \quad (9)$$

In making this estimate, we have explicitly included an estimate, using the single-particle model, with admixtures, of $\Delta(p_{1/2})/\Delta(s_{1/2}) \approx 0.363$. Then, from (8) and (9), we find

$${}^{195}\Delta^{199}(s_{1/2}) = 0.1684(118)\%. \quad (10)$$

DISCUSSION

Configuration Mixing Coefficients in the Nuclear Shell Model

The $s_{1/2}$ electron hyperfine anomaly (10) and the measured nuclear moments for a pair of isotopes provide three quantities that can now be interpreted in terms of the single-particle model of the nucleus with configuration mixing. Adopting the semiphenomenological approach suggested by Stroke and others,⁹ we try to obtain a fit of the experimental values for the anomaly and the moments of the pair of isotopes to the theoretical values for the μ_k and ${}^k\Delta^{199}$ based on the single-particle model with two admixed configurations in the nuclear wave function. For example, using the configuration mixing model, we can write the magnetic moment for a nucleus in a single-particle state of total angular momentum j and orbital angular momentum l ,

$$\mu_k = \mu_{s.p.}(l, j) + \sum_i \alpha_{0,k}^{(i)} (g_S^{(i)} - g_L^{(i)}). \quad (11)$$

Here $\mu_{s.p.}(l, j)$ is the single-particle or Schmidt value of the magnetic moment and the $\alpha_{0,k}^{(i)}$ are coefficients used by Stroke,⁹ which are proportional to the coefficients $\alpha_k^{(i)}$ for the admixed configurations in the nuclear wave function.¹⁰ We vary the $\alpha_k^{(i)}$ subject to the condition that $\sum_{k,i} |\alpha_k^{(i)}|^2 = \text{minimum}$, to get a fit to the data by using as little admixture as possible. The perturbation approach of Stroke and others⁹ and Arima and Horie¹⁰ is not satisfactory when the $|\alpha_k^{(i)}|$ get much larger than 0.1–0.2. The three isotopes of Hg with $I = \frac{1}{2}$ and the $I = \frac{3}{2}$ isotope (Hg²⁰¹) for which anomaly data are available can be fitted in this way with reasonable values of the admixture coefficients,

TABLE V. Admixture coefficients $\alpha_k^{(i)}$ obtained from magnetic moment and anomaly data on Hg isotopes.^a

| Isotope (<i>k</i>) | μ_k | $k\Delta^{199}$ | Nuclear spin | $(1h_{11/2})^{12} \rightarrow (1h_{9/2})^0$ and $(2d_{5/2})^6 \rightarrow (2d_{3/2})^2$ proton excitations admixed: | |
|-------------------------|---------|-----------------|-----------------|---|------------------|
| | | | | $\alpha_k^{(h)}$ | $\alpha_k^{(d)}$ |
| Hg ¹⁹⁶ | +0.5381 | +0.1684(118) | $\frac{1}{2}$ | -0.014(3) | +0.001(1) |
| Hg ¹⁹⁷ | +0.5241 | +0.0899(52) | $\frac{1}{2}$ | -0.009(2) | -0.014(5) |
| Hg ¹⁹⁹ | +0.5027 | ... | $\frac{1}{2}$ | -0.006(1) | -0.027(2) |
| Hg ²⁰¹ | -0.5567 | +0.1597(73) | $\frac{3}{2}$ | +0.004(0) | +0.294(0) |

^a The μ_k are diamagnetically corrected nuclear magnetic moments in nuclear magnetons (Refs. 6, 7) and the $k\Delta^{199}$ are the hfs anomalies for the $s_{1/2}$ electron in percent relative to Hg¹⁹⁹ [this paper and C. V. Stager, Phys. Rev. 132, 175 (1963)].

as shown in Table V. The two admixed configurations considered are the only ones permitting a fit to the data with small enough values of the admixture coefficient.⁹ In the absence of a detailed calculation of the $\alpha_k^{(i)}$ from nuclear theory, we can at least say that the configuration mixing theory is not inconsistent with the observed moments and anomalies for these isotopes. The $\alpha^{(i)}$ for the $I = \frac{1}{2}$ isotopes cannot be calculated by using the simple δ -function interaction of Arima and Horie,¹⁰ since this interaction gives $\alpha^{(i)} \equiv 0$ for a $p_{1/2}$ shell-model state. It may be feasible to calculate $\alpha^{(i)}$ for the $p_{1/2}$ isotopes by using a somewhat more complex effective nucleon-nucleon interaction³⁵ than the delta-function interaction.

ACKNOWLEDGMENTS

It is a pleasure to acknowledge the guidance and support of Professor Francis Bitter during the course of this work. Dr. H. R. Hirsch and Dr. H. H. Stroke were most helpful in the laboratory and in clarifying my understanding of level crossings and hyperfine anomalies. I am grateful for many stimulating discussions with Dr. Lee C. Bradley III, Dr. W. J. Tomlinson, III, and Dr. W. T. Walter.

I would like to thank A. Koehler and R. Wharton of the Cyclotron Group, Harvard University, for the bombardments. Some of the machine computations were performed at the Computation Center, M.I.T. I should also like to thank the National Bureau of Standards Boulder Laboratories for additional computational assistance.

APPENDIX A: SHIFTS IN THE CENTER OF A LEVEL-CROSSING CURVE CAUSED BY DEVIATIONS FROM EXACT 90° SCATTERING

The intensity change in the neighborhood of a crossing of two excited-state sublevels¹⁷ is given by

$$R(\mathbf{f}, \mathbf{g}) - R_0 = \frac{A + A^*}{1 + (\Delta\omega\tau)^2} + \frac{i(A - A^*)\Delta\omega\tau}{1 + (\Delta\omega\tau)^2}, \quad (\text{A1})$$

where $A = A(\mathbf{f}, \mathbf{g})$ is proportional to the product of four

³⁵ See, for example, F. Tabakin and F. Villars, Bull. Am. Phys. Soc. 9, 74 (1964).

electric-dipole matrix elements as defined by Franken,¹⁷ \mathbf{f} is the polarization vector of the incident light, \mathbf{g} the polarization vector of the scattered light, τ is the natural lifetime of the excited-state levels that cross, and $\Delta\omega = (E - E')/\hbar$ is a measure of the energy separation of the two atomic sublevels. As the applied magnetic field is swept through the crossing point, $\Delta\omega$ goes through zero, and an intensity change is observed in the scattered light. Whether the intensity increases or decreases in the neighborhood of the crossing and whether the line shape is pure Lorentzian, dispersion-shaped, or some mixture of the two, is determined by the sign of the quantity A and by whether A is real, imaginary or complex.

As an example, we assume that the incident and scattered polarization vectors both lie in a plane perpendicular to the applied magnetic field and that the angle between them is ϕ . From knowledge of the electric dipole matrix elements at the crossing field between the initial ground-state Zeeman sublevel and the two excited-state sublevels that cross, A can be computed as a function of the angle ϕ . For the case (see Fig. 2) of an atom with a 1S_0 ground state and 3P_1 excited state, having a nuclear spin $I = \frac{1}{2}$, we find

$$A \sim -(\sin^2\phi - \cos^2\phi + 2i \sin\phi \cos\phi). \quad (\text{A2})$$

If $\phi = 90$ or 180° , A is real and we have a Lorentzian line shape. If $\phi = 45$ or 135° , A is pure imaginary and we have a dispersion line shape. If, as is often the case in level-crossing experiments, A is close to but not exactly 90° , then some of the dispersion shape is mixed with the Lorentzian shape, with the result that there is a shift in the center of the line. It will be shown below how a set of level-crossing data may be corrected for small deviations from effective 90° scattering by estimating the asymmetry in the line accompanying the shift of the center.

Defining $x \equiv \Delta\omega\tau$, we rewrite (A1) as

$$R - R_0 = \frac{2 \operatorname{Re} A}{1 + x^2} - 2 \operatorname{Im} A \frac{x}{1 + x^2}. \quad (\text{A3})$$

For small-amplitude field modulation, the observed

line shape is proportional to the derivative of (A3):

$$\frac{d}{dx}(R-R_0) = -4 \operatorname{Re}A \frac{x}{(1+x^2)^2} - 2 \operatorname{Im}A \frac{1-x^2}{(1+x^2)^2}. \quad (\text{A4})$$

For exact 90° scattering, A is real and the line has a zero at $x=0$ and peaks at positions given by $x = \pm (\frac{1}{3})^{1/2}$. Both peaks have the same height, measured from the base line.

If the scattering is not exactly 90° , we have $\operatorname{Im}A \neq 0$, but instead $|\operatorname{Im}A| \ll |\operatorname{Re}A|$. The center of the line is now given by $-2 \operatorname{Re}Ax - \operatorname{Im}A(1-x^2) = 0$ or

$$x = \frac{-\operatorname{Im}A(1-x^2)}{2 \operatorname{Re}A} \approx -\frac{\operatorname{Im}A}{2 \operatorname{Re}A}. \quad (\text{A5})$$

The positive and negative peaks are now located at the positions

$$x^{(+)} \approx \frac{1}{\sqrt{3}} + \frac{1 - \operatorname{Im}A}{2 \operatorname{Re}A}, \quad (\text{A6})$$

$$x^{(-)} \approx -\frac{1}{\sqrt{3}} + \frac{1 - \operatorname{Im}A}{2 \operatorname{Re}A},$$

and the corresponding peak heights are

$$A \approx \left| -\frac{9}{4\sqrt{3}} \operatorname{Re}A - \frac{3}{4} \operatorname{Im}A \right|, \quad (\text{A7})$$

$$B \approx \left| \frac{9}{4\sqrt{3}} \operatorname{Re}A - \frac{3}{4} \operatorname{Im}A \right|.$$

If we define the resulting "asymmetry" by

$$\alpha \equiv \frac{B-A}{B+A} = \frac{1 - \operatorname{Im}A}{\sqrt{3} \operatorname{Re}A}, \quad (\text{A8})$$

we see that for small contributions to the line shape from $\operatorname{Im}A$ ($-\operatorname{Im}A/\operatorname{Re}A \ll 1$), the shift of the center of the line is related to the measured asymmetry by

$$x \approx \frac{\sqrt{3}}{2} \alpha \approx 0.866\alpha. \quad (\text{A9})$$

Putting this another way, if $\delta \ll 1$ is the small angular deviation from $\phi = \pi/2$, the shift, by using (A2),

$$x = \frac{1 - \operatorname{Im}A}{2 \operatorname{Re}A} = \frac{-\sin(\frac{1}{2}\pi + \delta) \cos(\frac{1}{2}\pi + \delta)}{\sin^2(\frac{1}{2}\pi + \delta) - \cos^2(\frac{1}{2}\pi + \delta)} \approx +\delta. \quad (\text{A10})$$

APPENDIX B: DETAILED PRESENTATION OF EXPERIMENTAL DATA

(Errors are one standard deviation of the measurements unless otherwise indicated.)

TABLE B.I. Hg^{199} level-crossing data: $F = \frac{3}{2}$, $m_F = -\frac{3}{2} \times F = \frac{1}{2}$, $m_F = \frac{1}{2}$. Weighted mean of all data = 30 197.95(36) kc for 93 peaks. The error quoted in Table I for this crossing in Hg^{199} is larger than three times the standard deviation of the mean. The error limits are chosen to encompass all four of the means given here. Thus, some of the uncertainty resulting from cell-to-probe corrections is included in this error estimate. Changes in the cell and probe positions from run to run are believed to account for most of the scatter between the various means.

| Run | Mean proton resonance frequency for crossing ^a (kc) | Number of peaks | Mean proton frequency corrected for asymmetry | Remarks |
|-----|--|-----------------|---|--|
| 1 | 30 197.86(26) | 15 | 30 197.76(30) | Intensity crossing, A pole pieces |
| 2 | 30 198.18(26) | 20 | 30 198.18(26) | Observed by using field modulation, A pole pieces |
| 3 | 30 197.80(46) | 19 | 30 197.80(46) | Observed by using field modulation, B pole pieces |
| 4 | 30 197.93(28) | 39 | 30 197.93(28) | Observed by using field modulation, B pole pieces. |

^a "Normalized means" presented in Table I are computed from the weighted means of the frequency ratios by multiplying by the mean proton resonance frequency for the Hg^{199} crossing: 30 197.95 kc/sec.

TABLE B.II. Radioactive level crossings observed

| Isotope and crossing | Run | Mean proton resonance frequency corrected for asymmetry (kc/sec) (see Hg^{199} data) | Number of peaks in run | Weighted mean of all data (kc/sec) | Ratio of proton resonance frequencies for each run $\nu[H_+] / \nu[H_+(199)]$ (Errors here are three times the standard deviation of the mean.) |
|--|------|---|------------------------|------------------------------------|---|
| 195 | | | | | |
| $(\frac{3}{2}, -\frac{3}{2}) \times (\frac{1}{2}, \frac{1}{2})$ | 1 | 32 369.86(34) | 79 | 32 369.95(38) | 1.071929(12) |
| | 2 | 32 370.30(33) | 20 | | 1.071929(13) |
| 195* | | | | | |
| $(\frac{15}{2}, \frac{15}{2}) \times (\frac{13}{2}, \frac{11}{2})$ | 1 | 33 925.86(37) | 31 | 33 926.78(63) | 1.123456(15) |
| | 2 | 33 926.93(40) | 42 | | 1.123476(14) |
| 195* | | | | | |
| $(\frac{13}{2}, \frac{11}{2}) \times (\frac{13}{2}, \frac{7}{2})$ | 2 | 32 682.7(9) | 18 | 32 682.7(9) | 1.082278(27) |
| 195* | | | | | |
| $(\frac{13}{2}, \frac{9}{2}) \times (\frac{13}{2}, \frac{5}{2})$ | 2 | 31 580.7(70) | 6 | 31 580.7(70) | ... |
| 193* | | | | | |
| $(\frac{15}{2}, \frac{15}{2}) \times (\frac{13}{2}, \frac{11}{2})$ | 3 | 34 380.54(48) | 8 | 34 380.51(38) | 1.138511(26) |
| | 4(a) | 34 380.36(19) | 11 | | 1.138505(12) |
| | 4(b) | 34 380.84(34) | 9 | | |
| | 4(c) | 34 380.59(29) | 10 | | |

APPENDIX C: A METHOD FOR MEASURING SMALL
MAGNETIC FIELD DIFFERENCES IN THE
PRESENCE OF FIELD FLUCTUATIONS

Gabillard³⁶ has shown that if one looks at the envelope of a fast-passage proton resonance induction signal when the inhomogeneities over the sample are fairly large ($\langle \Delta H \rangle_{av} \gtrsim 1/\gamma T_2$, where T_2 is the transverse relaxation time), what one sees is not a simple exponential decay of the side wiggles, but an exponential decay that is modulated by the Fourier transform of the field distribution over the sample. This modulation is the result of beats between the induction signal from various parts of the sample which have slightly different Larmor precession frequencies, and the oscillator voltage in the coil. Thus, we can write for the envelope of the nuclear induction signal

$$V(t) = V_0 e^{-t/T_2} F(t), \quad (C1)$$

with $F(t) = \int_{-\infty}^{\infty} e^{i\gamma\delta t} \phi(\delta) d\delta$, where $\delta \equiv H - H_0$, γ is the proton gyromagnetic ratio, and $\phi(\delta)$ is the distribution of inhomogeneities. Gabillard considered the case in which the magnetic field varies linearly across the sample, that is

$$\begin{aligned} \phi(\delta) &= 0, & |\delta| > \Delta \\ &= \text{constant}, & |\delta| \leq \Delta. \end{aligned}$$

Then we have

$$\begin{aligned} F(t) &\sim 2 \int_0^{\Delta} \cos \gamma \delta t d\delta \\ &= 2\Delta (\sin \gamma \Delta t / \gamma \Delta t). \end{aligned} \quad (C2)$$

The separation between zeros (or maxima) of $F(t)$ then gives a measure of the inhomogeneity parameter Δ .

This effect can be used to measure small magnetic field differences (for example, the cell-to-probe correction in a level-crossing experiment) in the following way. Separate small magnetic-resonance probes are placed at the two positions to be monitored and connected in parallel to the oscillator. If the fields at the two probes are $H_0 \pm \Delta$ and are homogeneous over the volume of each probe, we can write $\phi(\delta)$ as a sum of two δ functions: $\phi(\delta) \sim \delta(\delta + \Delta) + \delta(\delta - \Delta)$, which gives

$$F(t) \sim 2 \cos \gamma \Delta t. \quad (C3)$$

³⁶ See P. Grivét, *La Résonance Paramagnétique Nucléaire* (Centre National de la Recherche Scientifique, Paris, 1955), pp. 137 and 145.

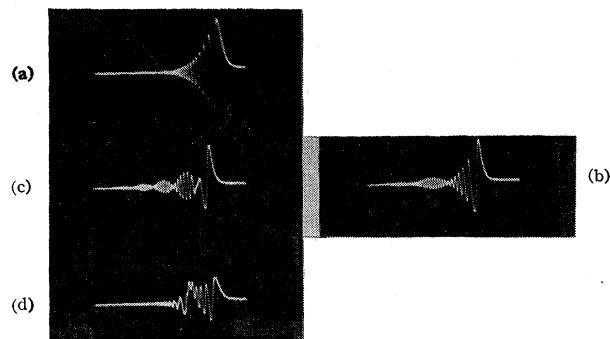


FIG. 7. Effect of increasing increments in small magnetic field differences on side wiggles in nuclear magnetic resonance, using two probes connected in parallel. (A quantitative analysis of these beat patterns is difficult when there is appreciable inhomogeneity over the sample volume of one probe.)

Measuring the time between successive zeros of the nuclear induction envelope by using an oscilloscope with calibrated time base gives the value of the field difference Δ . We note that (C2) represents essentially a single-slit diffraction pattern, while (C3) is a double-slit pattern. In any practical case there would be small inhomogeneities over the volume of each probe, so the "double-slit" pattern (C3) would have a "single-slit" envelope. This makes the interpretation of the patterns difficult when one attempts to measure field differences as small as the inhomogeneities over the probe volume.

The technique just described seems to have the advantage that one can measure field differences that are somewhat smaller than the linewidth of the nuclear resonance signal. Furthermore, if there are random fluctuations in the fields at each of two probes such that the field difference remains nearly constant, the beat pattern may still be observable. This was the reason the method was thought to be applicable to the present experiment, in which fluctuations in magnet current produced field fluctuations comparable in size to the differences to be measured. Inhomogeneities over the volume of the rather large probes that were used made it impossible to get good measurements of the field difference (see above). Some of the patterns observed are shown in Fig. 7. This "beat-pattern method" would be particularly useful if one were trying to set the fields in two separate magnets equal with high precision.

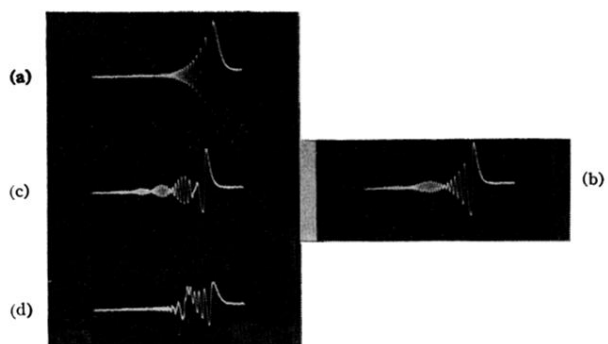


FIG. 7. Effect of increasing increments in small magnetic field differences on side wiggles in nuclear magnetic resonance, using two probes connected in parallel. (A quantitative analysis of these beat patterns is difficult when there is appreciable inhomogeneity over the sample volume of one probe.)